The Use of Triquaternary Alkylammonium Ions in the Synthesis of STA-5, a Magnesioaluminophosphate with the BPH Framework Topology

Veronique Patinec,[†] Paul A. Wright,*[,†] R. Alan Aitken,[†] Philip Lightfoot,[†] Stuart D. J. Purdie,[†] Paul A. Cox,[‡] Åke Kvick,[§] and Gavin Vaughan[§]

School of Chemistry, University of St. Andrews, The Purdie Building, North Haugh, St. Andrews, Fife, KY16 9ST, U.K., Division of Chemistry, University of Portsmouth, St. Michael's Building, White Swan Road, Portsmouth, PO1 2DT, U.K., and ESRF, BP220, 38043 Grenoble, CEDEX, France

Received March 15, 1999. Revised Manuscript Received June 18, 1999

The triquaternary organic cations 1,3,5-Tris(triethylammoniomethyl)benzene (**1**) and 1,3,5-Tris(quinuclidiniomethyl)benzene (**2**) were synthesized and used as structure-directing agents in the synthesis of magnesioaluminophosphates (MAPOs). **2** Results in the preparation of STA-1, a known structure composed of intersecting large pore channels, whereas **1** results in the synthesis of STA-5, a MAPO with the BPH topology. The structure of STA-5, which contains a one-dimensional cage and channel structure limited by 12-membered rings, was solved using powder X-ray data and confirmed by microcrystal diffraction at a synchrotron source. STA-5 has trigonal symmetry, space group *P*321, $a = 13.221(1)$ Å, $c = 13.339(1)$ Å. The template was found to be incorporated intact, and by a combination of computation and diffraction, was found to fill space effectively in the channel, with nearly every supercage being occupied by a template molecule. Upon calcination in oxygen at 550 °C, the template is removed, leaving the framework of STA-5 intact.

Introduction

The use of alkylammonium ions as templates for the crystallization of molecular sieves remains an area of intense and fruitful research activity, the aim being the synthesis of a wide range of framework topologies with shape-selective catalytic and adsorption properties.[1−6] Our approach to extending this range is to design and synthesize organic bases likely, on the basis of their shape and size, to template new and useful inorganic structures. By far the majority of templates, or structure-directing agents, that have been reported to successfully generate new structures have been monoquaternary or diquaternary alkylammonium salts. Only one triquaternary template, 2,3,4,5,6,7,8,9-octahydro-2,2,5,5,8,8-hexamethyl-1H-benzo[1,2-c:3,4-c′:5,6-c″] tripyrrolium ("triquatP"), has been reported to template a new "zeotype",[7] and the "triquat"-ZSM-18 system is frequently referred to as one of the best examples of true templating. In that case the organic cation−zeolite framework fit is a precise one, where the cation has an exact symmetry match to the supercage in which it is located.

We initiated studies on the use of triquaternary templates in the synthesis of magnesioaluminophosphates (MAPOs)—the presence of magnesium in the framework results in a negatively charged framework that is charge-balanced by organic cations. In addition to imparting solid acidity to the microporous frameworks, it also has the effect of accelerating the crystallization. In particular, we prepared organic cations that are based on a trisubstituted benzene ring. One of the challenges in aluminophosphate synthesis is to prepare large pore solids with topologies other than that possessed by AlPO-5-type materials (structure code AFI),[8] which is readily prepared under a wide range of conditions. If the triquaternary organic cations we prepared and used in synthesis are incorporated intact, magnesioaluminophosphate-5 (MAPO-5) will not result, because the channels are too narrow to accommodate the cations, and the resulting frameworks will necessarily have large cavities within them. We report here the successful synthesis of large pore magnesioaluminophosphates other than MAPO-5 using this approach, including the novel STA-5, but cocrystallization of MAPO-5 remains an important consideration.

Experimental Section

Triquaternary templates **1** and **2** (Scheme 1) were prepared by heating a solution of 1,3,5-tris(bromomethyl)benzene[9] (1.25

* Address correspondence to: Dr. Paul Wright (E-mail: paw2@st-andrews.ac.uk. Tel.: 01334-463793. Fax: 01334-463808).
† University of St. Andrews.
‡ University of Portsmouth.
§ ESRF.

(1) Barrer, R. M.; Denny, P. J. *J. Chem. Soc.* **1961**, 971.
(2) Wilson, S. T.; Lok, B. M.; Messina, C. A.; Cannan, T. R.; Flanigen, E. M. *J. Am. Chem. Soc.* **1982**, *104*, 1146.
(3) Shannon, M. D.; Casci, J. L.; Cox, P. A.; Andrews, S. J. *Nature* **1991**, *353*, 417.
(4) Zones, S. I.; Nakagawa, Y.; Yuen, L. T.; Harris, T. V. *J. Am. Chem. Soc.* **1996**, *118*, 7558.
(5) Noble, G. W.; Wright, P. A.; Lightfoot, P.; Morris, R. E.; Hudson, K. J.; Kvick, Å.; *Angew. Chem., Int. Ed. Engl.* **1997**, *36*, 81.
(6) Noble, G. W.; Wright, P. A.; Kvick, Å. *J. Chem. Soc., Dalton Trans.* **1997**, 4485.
(7) Lawton, S. L.; Rohrbaugh, W. J. *Science* **1990**, *24*, 1319.
(8) *Atlas of Zeolite Structure Types*, 4th Revised ed.; Meier, W. M., Olson, D. H., Baerlocher, Ch., Eds.; Elsevier: New York, 1996; p 26.

10.1021/cm991032s CCC: $18.00
Published on Web 08/19/1999

Scheme 1

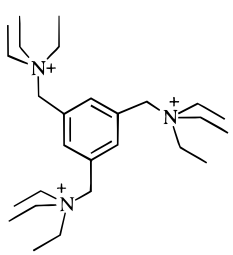

1

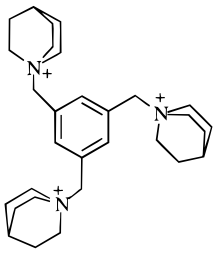

2

g, 3.5 mmol) and the corresponding amine (10.5 mmol) in ethanol (30 mL) under reflux for 5 h.

Evaporation followed by recrystallization of the residue from acetonitrile/ethanol (3:1) gave products as follows. 1,3,5-Tris-(triethylammoniomethyl)benzene tribromide (**1**): Reaction using triethylamine. Yield = 79%; mp > 300 °C; ^{1}H NMR (D_2O) δ 7.74 (s, 3H, C_6H_3), 4.57 (s, 6H, CH_2−Ar), 3.28 (q, 18H, CH_2CH_3, J = 7 Hz), 1.44 (t, 27 H, CH_3, J = 7 Hz); ^{13}C NMR (D_2O) δ 136.2, 127.8, 56.7 (CH_2−Ar), 50.7 (CH_2CH_3), 5.2 (CH_3). Anal. Calcd for $C_{27}H_{54}N_3Br_3 \cdot H_2O$: C, 47.79; H, 8.32; N, 6.19. Found: C, 47.83; H, 8.40; N, 6.18. 1,3,5-Tris(quinuclidiniomethyl)benzene tribromide (**2**): Reaction using quinuclidine. Yield = 85%; mp > 300 °C; ^{1}H NMR (D_2O) δ 7.93 (s, 3H, C_6H_3), 4.57 (s, 6H, CH_2−Ar), 3.72 (t, 18H, NCH_2CH_2, J = 7.7 Hz), 2.20 (t, 3H, CH, J = 3 Hz), 2.07 (m, 18H, NCH_2CH_2); ^{13}C NMR (D_2O) δ 140.7, 130.8, 67.3 (CH_2−Ar), 55.7 (NCH_2-CH_2), 24.9 (NCH_2CH_2), 21.4 (CH). Anal. Calcd for $C_{30}H_{48}N_3$-$Br_3 \cdot H_2O$: C, 50.86; H, 7.12; N, 5.93. Found: C, 50.96; H, 7.25; N, 5.90.

The bromides were converted to the hydroxide form by exchange with silver oxide and used as structure-directing agents in the synthesis of MAPOs by the sequential addition of aluminum hydroxide, magnesium acetate tetrahydrate, orthophosphoric acid, and the template hydroxide to distilled water using a mole ratio of 0.85:0.15:1.0:0.4:40. Once prepared, the gel was transferred to a stainless steel, poly(tetrafluoroethylene) (PTFE)-lined autoclave and heated under hydrothermal conditions at temperatures between 110 and 190 °C. The syntheses at 190 °C resulted in crystals of a range of sizes, including STA-1 and STA-5 single crystals with dimensions up to 40 μm which could be separated from the smaller crystals by sonication. Characterization of the MAPO products was performed initially using X-ray powder diffraction using Cu $K\alpha_1$ radiation on a STOE STADIP laboratory diffractometer with a primary monochromator. Data were collected from 5 to 70° 2θ with a step size of 0.02° 2θ. A single microcrystal of STA-5, a hexagonal platelet 40 μm wide and 10 μm thick, was examined using the single-crystal facility at the ID-11 beamline at the ESRF, Grenoble. The microcrystal was glued to the end of a fine glass fiber and data were collected at room temperature on a three-circle (fixed kappa) Siemens diffractometer fitted with a Siemens SMART CCD detector. The wavelength was calibrated prior to the experiment as 0.3754 Å. Data were collected in ω steps of 0.1° over 140°, with the detector 2θ and goniometer ϕ circles fixed. Data were collected for d spacings less than 4.0 Å and the resolution limit was 0.45 Å. Data reduction was carried out using the Bruker AXS SAINT and SADABS packages. Data merging in $P321$ reduced the 27 642 recorded data to 7957 merged data and 1194 observed according to the criterion $I > 3\sigma(I)$. The basic framework structure was solved using the SHELXS package and refined using the TEXSAN suite. Full anisotropic refinement of 127 parameters produced residuals of $R(F) = 12.8\%$, $R_w(F) = 10.8\%$, but it was not possible to identify template molecules from the difference Fourier synthesis.

Computer simulations of the template position were performed by a combination of Monte Carlo generation of different template conformations and docking of these into the $AlPO_4$ framework. Subsequently, the energy of template molecules inside the pore structure was minimized using the consistent valence force field within the program Discover[10] using simulated annealing.

Table 1. The Results of Hydrothermal Syntheses Using Gel Compositions and Templates as Described in the Text, as a Function of Crystallization Temperature

template	pH	temperature (°C)	time (h)	product
1	8	160	72	STA-5, MAPO-5, unknown phase
1	8	190	24	STA-5, MAPO-5
2	8	160	72	layered phase
2	8	190	24	STA-1, MAPO-5

Further characterization of bulk samples was performed by chemical analysis, NMR, and thermogravimetric analysis. The inorganic chemical analysis of the microcrystalline fraction of STA-5 was performed by inductively coupled plasma−atomic emission spectroscopy (ICP−AES) on a sample that had been dissolved in nitric acid after fusion with $LiBO_2$. Carbon, hydrogen, and nitrogen analysis was performed in order to determine the amount and composition of the organic component in as-prepared samples of STA-1 and STA-5. ^{13}C cross-polarization/magic angle spinning (CP MAS) NMR spectra were obtained using a Bruker MSL 500 spectrometer at 125.758 MHz. The following typical conditions were employed: contact time 1 ms, recycle delay 5 s, spinning speeds 6−8 kHz. Chemical shifts were referenced to the CH_2 resonance in an external adamantane sample at 38.56 ppm. ^{31}P and ^{27}Al MAS NMR of STA-5 were collected using the MSL 500 spectrometer and chemical shifts were referenced to an 85 wt % solution of H_3PO_4 and to $[Al(H_2O)_6]^{3+}$, respectively. Thermogravimetric analysis of STA-5 was performed in oxygen using a heating rate of 5 °C/min up to 600 °C.

To investigate the stability of the product MAPOs upon removal of the template, samples were calcined at 550 °C in flowing dry oxygen for 8 h. Upon subsequent cooling below 200 °C the gas stream was switched to dry nitrogen saturated with cyclohexane vapor at room temperature. This permits the channels to become filled with adsorbed organic molecules and inhibits the subsequent adsorption of water upon exposure to moist air, which is known to cause distortion and structural degradation in related aluminophosphate structures.

Results

The crystalline products of hydrothermal syntheses using the two templates are shown in Table 1. The triquinuclidinium template results in the formation of a mixture of the known phases STA-1[5] and MAPO-5 at 190 °C and of an unidentified and imperfectly crystalline phase at 160 °C, the diffraction pattern of which is dominated by a reflection with a d spacing of 14.1 Å. The tris(triethylamine) triquat results in the formation of the new phase STA-5 at both 160 and 190 °C, in association with other phases, particularly MAPO-5. The relative amounts of STA-5 and MAPO-5 in the preparation, even under very similar conditions, are very variable, indicating that the undesired competitive crystallization of MAPO-5 is difficult to prevent. In one preparation at 160 °C STA-5 was prepared in the absence of MAPO-5 but together with a small amount of another, unidentified phase, and we examined the STA-5 from this preparation in detail below. It was possible to achieve mixtures enriched in STA-1 and STA-5 by physical methods (sonication and decanting) so that nearly phase pure samples of STA-1 and STA-5 could be obtained.

(9) Cochrane, W. P.; Pauson, P. L.; Stevens, T. S. *J. Chem. Soc. C* **1968**, *630*.

(10) DISCOVER 3.1 Program, MSI, San Diego, CA.

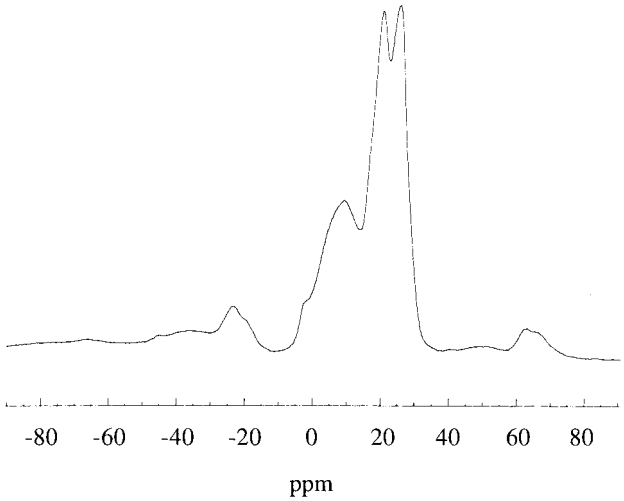

Figure 1. ^{31}P MAS NMR of a sample of STA-5, which contains less than ca. 10% of a crystalline impurity phase. The spectrum is dominated by two sharp resonances, at −20.5 and −25.2 ppm, and a broad resonance at −10.0 ppm.

^{27}Al MAS NMR indicates that both samples have predominantly tetrahedral aluminum although small amounts of aluminum in octahedral coordination are observed (STA-1, δ −41.3(strong), −2(weak); STA-5, δ −40.5(s), −2.0 (medium/weak)). This indicates that most of the aluminum in both structures is within a tetrahedrally connected framework. The octahedral aluminum in the STA-5 could be from unreacted aluminophosphate gel, because the sample examined was the fine fraction after sonication. For STA-1 the coarse fraction was taken because it contained only STA-1 crystals.

^{31}P MAS NMR of both STA-1 and STA-5 show sharp resonances between −19 and −27 ppm, which are consistent with tetrahedral phosphorus surrounded by different numbers of Mg and Al in their second nearest neighbor spheres, as discussed by Akolekar and Howe.[11] For the novel STA-5, the ^{31}P MAS NMR (Figure 1) possesses two sharp peaks, δ −20.5 and −25.2, with a broad peak at −10.0 ppm. On the basis of data presented in ref 11, the compositional data would be consistent with the two sharper peaks being from phosphorus surrounded by 3Al, 1Mg, and 4Al in their second nearest neighbor coordination shells. It is more difficult to assign the broader peak.

C, H, and N analysis and ^{13}C MAS NMR, taken together, indicate that template molecules in STA-1 and STA-5 phases are included intact. For STA-1 the C, H, and N values (on the basis of N) for the organic molecules within the solid are close to those expected for the triquaternary ion ($C/H/N_{expected}$ = 30:48:3, $C/H/N_{measured}$ = 30:58:3 (extra H from occluded water) and the ^{13}C MAS NMR spectrum shows resonances at 138.9 and 129.6 ppm for the aromatic carbons; 68.7 ppm for the methylene groups; and 56.2, 24.7, and 20.8 ppm for quinuclidinium carbons, which correspond well to those observed in solution (see Experimental Section). For STA-5 the chemical analysis again agrees ($C/H/N_{expected}$ = 27:54:3, $C/H/N_{measured}$ = 27:80:3) and the ^{13}C MAS NMR resonances are consistent with the triquaternary molecules being retained intact (δ 138.7, 130.7, 71.6, 54.8, and 8.6). NMR of MAPO-5 formed with the tris-triethylamine triquaternary template under very similar conditions reveals that the included organic species is triethylamine (δ 47.6 and 8.8).

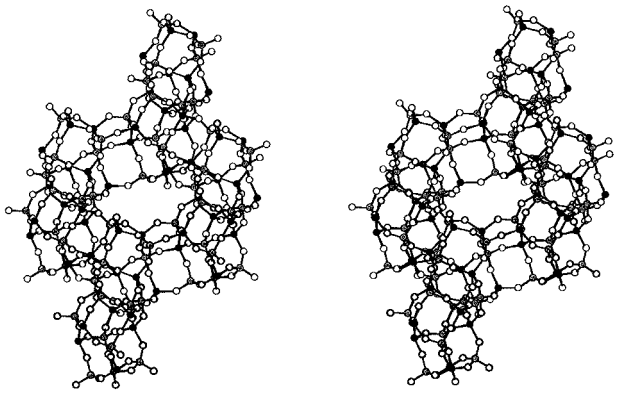

Figure 2. Stereoview of the aluminophosphate sheets common to STA-5 and MAPO-46. The tetrahedral cations aluminum (black) and phosphorus (gray) are linked by oxygens (white). The two structures differ mainly in the mode of stacking of these sheets.

The Framework Structure of STA-5. Initial examination of the X-ray powder diffraction profile of the bulk sample of STA-5 revealed similarities with that reported for the structure type MAPO-46[12] and it was found that the observed reflections (other than some very small peaks attributed to an unidentified impurity phase) could be indexed on a unit cell very similar to that of MAPO-46. However, Rietveld profile refinement using the framework coordinates of MAPO-46 was unable to fit the diffraction pattern closely (R_{wp} = 34%). At first it was thought this could be a result of neglecting the scattering from the triquaternary template, so the energetically favored position of the template molecule was generated by computational methods and included into the refinement, an approach that works well in many other examples. However, in this case, no improvement of the fit was obtained and it was concluded that the material does not possess the MAPO-46 topology. Closer examination of the MAPO-46 (structure code AFS) showed that adjacent aluminophosphate sheets that make up the MAPO-46 structure (Figure 2) may be stacked in two different ways. In the AFS case each sheet is rotated by 60° with respect to that below—because the sheet has 3-fold symmetry, this results in a *c*-axis repeat of around 26.9 Å. Alternatively, the sheets can be stacked one upon the other in the same orientation, giving a repeat unit of around 13.4 Å. Study of the literature revealed that the alternative topology was observed previously with beryllophosphate[13] and aluminosilicate[14] compositions, and was given the BPH structure code, but to our knowledge a magnesium aluminophosphate with this topology has not been prepared previously. Using framework coordinates derived from the asymmetric unit of MAPO-46 by appropriate choice of asymmetric unit and using

(11) Akolekar, D. B.; Howe, R. F. *J. Chem. Soc., Faraday Trans.* **1997**, *93*, 3263.

(12) *Atlas of Zeolite Structure Types*, 4th Revised ed.; Meier, W. M., Olson, D. H., Baerlocher, Ch., Eds.; Elsevier: New York, 1996; p 32.

(13) Harvey, G.; Baerlocher, Ch.; Wroblewski, T. *Z. Kristallogr.* **1992**, *201*, 113.

(14) Andries, K. J.; Bosmans H. J.; Grobet, P. J. *Zeolites* **1991**, *11*, 124.

space group symmetry *P*321 of the BPH structure, and refining unit cell and instrumental parameters only, we achieved a much better fit to the X-ray powder data. The possibility that the bulk powder sample could be a mixture of MAPO-46 and a MAPO with the BPH topology was then considered. The doubled *c*-axis of the MAPO-46 structure (*P*3*c*1, $a = 13.2$, $c = 26.89$ Å[12]) compared with the MAPO−BPH structure (*P*321, $a = 13.2$, $c = 13.34$) results in reflections of the type *hkl*, where *l* is odd for the MAPO-46 structure, which cannot occur for the MAPO−BPH structure. For example, the ⟨111⟩, ⟨113⟩, and ⟨123⟩ reflections of MAPO-46 occur at Bragg angles where no reflections are expected for the MAPO−BPH structures (13.8, 16.7, and 22.8° 2θ) and have sufficiently high relative intensities (as observed and simulated[12]) to be observed if any crystals of MAPO-46 are present. No intensity is observed in these regions (see Figures 5 and 7) so that the sample under investigation is thought to contain no MAPO-46. Diffraction peaks at 7.4, 19.25, 22.3, and 33.35° 2θ that are due to an impurity phase (not MAPO-46) were excluded in the final refinement.

Confident that STA-5 indeed possesses the BPH topology, we performed energy minimization of a hypothetical pure aluminophosphate structure using the potentials derived by Gale and found to simulate AlPO structures accurately.[15] The results of this energy minimization are given in Table 2a. Subsequently, single-crystal diffraction on hexagonal microcrystals showed these (see Experimental Section) to have the same structure as the bulk microcrystalline sample, and the framework coordinates are compared with the simulated values for the hypothetical AlPO framework in Table 2. Table 3 lists framework bond distances and angles from the STA-5 structure in Table 2c. Attempts to locate template molecules from the single-crystal data were unsuccessful. The channel structure of STA-5 is one-dimensional, with supercages connected via constrictions bounded by 12-membered rings (Figure 3). Connection between adjacent channels is possible via pores limited by eight-membered rings.

Template Location in STA-5. To discover the location of the triquaternary ammonium cation in the pores of STA-5, template-framework docking studies were performed using the Monte Carlo docking-simulated annealing methods described in the Experimental Section. Two types of low energy sites for the templates were found, and are illustrated in Figures 4a and b. In the first and lower energy location, the cation is positioned so that the benzene nucleus is oriented with its plane almost parallel to the *c*-axis of STA-5, with two of the $-N^+(C_2H_5)_3$ groups nestling into the "pockets" of the $AlPO_4$ framework at the side of the supercage and the third pointing up into the space between supercages. In the second case, the benzene nucleus is oriented perpendicular to the *c*-axis and all three of the $-N^+(C_2H_5)_3$ groups coordinate within the "sidepockets". In this way the cage and the triquaternary cation have matching 3-fold symmetry and there is excellent packing in the *ab* plane, but the calculated energy is less favorable because the "template"-framework fit is very tight and this leads to unreasonable distortions of the benzene ring and the benzylic carbons away from planarity.

To determine whether X-ray diffraction could differentiate between these models, they were used as starting points for the single-crystal diffraction data. Inclusion of the first template position (disordered over six equivalent positions, each with one-sixth occupancy) resulted in a slight improvement in the fit, $R(F)$ decreasing by 0.8% ($R(F) = 12.0\%$, $R_w(F) = 10.8\%$) whereas inclusion in the second orientation gave $R(F) = 12.8\%$, $R_w(F) = 10.8\%$. A much larger effect was observed during Rietveld refinement of the powder

Table 2. Fractional Coordinates of Framework Atoms in As-Prepared STA-5, as Determined by (a) Simulation of the $AlPO_4$ Framework, (b) Constrained Refinement of Powder Diffraction Data, and (c) Single Microcrystal Diffraction

a. Simulated Framework Coordinates

atom	*x*	*y*	*z*
P(1)	0.3333	0.6667	0.1168
P(2)	0.8656	0.5164	0.2638
P(3)	0.1365	0.4361	0.3819
Al(1)	0.6667	0.3333	0.1275
Al(2)	0.1388	0.6439	0.2640
Al(3)	0.8682	0.3101	0.3806
O(1)	0.7966	0.4516	0.1706
O(2)	0.3433	0.5632	0.1561
O(3)	0.4049	0.3970	0.2348
O(4)	0.5874	0.8087	0.3248
O(5)	0.4467	0.5993	0.3470
O(6)	0.8134	0.5851	0.3101
O(7)	0.8546	0.4273	0.3430
O(8)	0.0115	0.3408	0.3605
O(9)	0.3333	0.6667	0.0037
O(10)	0.5547	0.7168	0.4933

b. Constrained Rietveld Refinement of X-ray Powder Data

atom	*x*	*y*	*z*	U_{iso}/(Å)
P(1)	0.3333	0.6667	0.1130(17)	0.026
P(2)	0.8627(14)	0.5177(12)	0.2581(13)	0.026
P(3)	0.1395(15)	0.4369(15)	0.3827(14)	0.026
Al(1)	0.6667	0.3333	0.1291(17)	0.026
Al(2)	0.1346(13)	0.6460(14)	0.2507(15)	0.026
Al(3)	0.8575(17)	0.2991(12)	0.3798(15)	0.026
O(1)	0.7986(6)	0.4555(6)	0.1624(15)	0.030
O(2)	0.3531(6)	0.5650(6)	0.1441(15)	0.030
O(3)	0.3908(15)	0.3807(11)	0.2279(14)	0.030
O(4)	0.5746(13)	0.7904(13)	0.3096(15)	0.030
O(5)	0.4573(13)	0.5907(14)	0.3326(16)	0.030
O(6)	0.8266(16)	0.5942(14)	0.3140(16)	0.030
O(7)	0.8428(24)	0.4135(19)	0.3270(16)	0.030
O(8)	0.0086(16)	0.3591(15)	0.3634(14)	0.030
O(9)	0.3333	0.6667	−0.0002(16)	0.030
O(10)	0.5449(20)	0.7208(17)	0.4922(14)	0.030

c. Single-Crystal Data

atom	*x*	*y*	*z*	*B*(eq)/(Å^2)
P(1)	0.3333	0.6667	0.1221(9)	2.5(2)
P(2)	0.8639(7)	0.5155(7)	0.2642(5)	2.9(2)
P(3)	0.1352(7)	0.4378(7)	0.3813(5)	2.7(2)
Al(1)	0.6667	0.3333	0.1219(9)	2.0(2)
Al(2)	0.1370(7)	0.6455(7)	0.2685(6)	3.8(2)
Al(3)	0.8658(8)	0.3087(8)	0.3809(6)	3.1(2)
O(1)	0.790(2)	0.453(2)	0.168(1)	3.7(6)
O(2)	0.343(3)	0.567(3)	0.159(1)	5.6(8)
O(3)	0.398(2)	0.387(2)	0.241(2)	4.6(6)
O(4)	0.592(2)	0.806(2)	0.322(1)	3.5(5)
O(5)	0.440(2)	0.587(2)	0.354(1)	5.2(7)
O(6)	0.812(2)	0.593(2)	0.313(1)	3.3(5)
O(7)	0.851(2)	0.422(2)	0.340(1)	3.6(5)
O(8)	0.014(2)	0.341(2)	0.367(1)	4.5(6)
O(9)	0.3333	0.6667	0.006(2)	3.7(4)
O(10)	0.559(2)	0.721(2)	0.490(2)	5.4(6)

(15) Henson, N.; Cheetham, A. K.; Gale, J. D. *Chem. Mater.* **1996**, *8*, 664.

Table 3. Framework Bond Distances (Å) and Angles (deg) from STA-5 Structure Given in Table 2(c)

P(1)−O(2)	1.48(2)	Al(1)−O(1)	1.74(2)
P(1)−O(2)	1.48(2)	Al(1)−O(1)	1.74(2)
P(1)−O(2)	1.48(2)	Al(1)−O(1)	1.74(2)
P(1)−O(9)	1.55(3)	Al(1)−O(9)	1.69(3)
av. P(1)−O	1.50(3)	av. Al(1)−O	1.73(2)
P(2)−O(1)	1.57(2)	Al(2)−O(2)	1.81(2)
P(2)−O(3)	1.52(2)	Al(2)−O(3)	1.78(2)
P(2)−O(6)	1.63(2)	Al(2)−O(4)	1.78(2)
P(2)−O(7)	1.54(2)	Al(2)−O(5)	1.66(2)
av. P(2)−O	1.56(4)	av. Al(2)−O	1.76(5)
P(3)−O(4)	1.51(2)	Al(3)−O(6)	1.69(2)
P(3)−O(5)	1.59(2)	Al(3)−O(7)	1.70(2)
P(3)−O(8)	1.50(2)	Al(3)−O(8)	1.79(2)
P(3)−O(10)	1.49(2)	Al(3)−O(10)	1.76(2)
av. P(3)−O	1.52(4)	av. Al(3)−O	1.74(4)
O(2)−P(1)-O(2)	110(1)	O(1)−Al(1)-O(1)	108(1)
O(2)−P(1)−O(2)	110(1)	O(1)−Al(1)−O(1)	108(1)
O(2)−P(1)−O(2)	110(1)	O(1)−Al(1)−O(1)	108(1)
O(2)−P(1)−O(9)	109(1)	O(1)−Al(1)−O(9)	111(1)
O(2)−P(1)−O(9)	109(1)	O(1)−Al(1)−O(9)	111(1)
O(2)−P(1)−O(9)	109(1)	O(1)−Al(1)−O(9)	111(1)
av. O−P(1)−O	109.5(0.5)	av. O−Al(1)−O	109.5(1.5)
O(1)−P(2)−O(6)	108(1)	O(2)−Al(2)−O(3)	114(1)
O(1)−P(2)−O(7)	108(1)	O(2)−Al(2)−O(4)	108(1)
O(1)−P(2)−O(3)	113(1)	O(2)−Al(2)−O(5)	110(1)
O(3)−P(2)−O(6)	104(1)	O(3)−Al(2)−O(4)	104(1)
O(3)−P(2)−O(7)	113(1)	O(3)−Al(2)−O(5)	112(1)
O(6)−P(2)−O(7)	109(1)	O(4)−Al(2)−O(5)	110(1)
av. O−P(2)−O	109.2(3.0)	av. O−Al(2)−O	109.7(3.0)
O(4)−P(3)−O(5)	115(1)	O(6)−Al(3)−O(7)	111(1)
O(4)−P(3)−O(8)	107(1)	O(6)−Al(3)−O(8)	108(1)
O(4)−P(3)−O(10)	109(1)	O(6)−Al(3)−O(10)	110(1)
O(5)−P(3)−O(8)	112(1)	O(7)−Al(3)−O(8)	110(1)
O(5)−P(3)−O(10)	107(1)	O(7)−Al(3)−O(10)	114(1)
O(8)−P(3)−O(10)	107(1)	O(8)−Al(3)−O(10)	104(1)
av. O−P(3)−O	109.5(3.0)	av. O−Al(3)−O	109.5(3.0)
P(2)−O(1)−Al(1)	146(1)	P(2)−O(6)−Al(3)	132(1)
P(1)−O(2)−Al(2)	146(1)	P(2)−O(7)−Al(3)	155(1)
P(2)−O(3)−Al(2)	145(1)	P(3)−O(8)−Al(3)	141(1)
P(3)−O(4)−Al(2)	134(1)	P(1)−O(9)−Al(1)	180
P(3)−O(5)−Al(2)	149(2)	P(3)−O(10)−Al(3)	154(1)

X-ray data. The goodness of fit (R_{wp}) was determined for each template-framework model by first keeping the simulated coordinates of template and framework constant and allowing the template occupancy and instrumental and lattice parameters to vary, and then by permitting the framework atom positions to be refined, keeping the P−O and Al−O bond lengths constrained. The results show a much better fit for the template location with the benzene ring nearly parallel rather than perpendicular to the *c*-axis. (For the first case the R_{wp} value is improved to 9.7%, whereas for the second case R_{wp} remains high at 16.7%—the profile fit for the first case is given in Figure 5). Both simulation and X-ray diffraction therefore indicate that the first template orientation is that adopted in the structure. It was not possible to unambiguously locate water molecules from the difference Fourier syntheses. The efficient space filling of the template of the supercage and channel system is shown in Figure 6.

Combined diffraction, NMR, and chemical analysis indicate a unit cell composition of $Mg_{2.1}Al_{11.9}P_{14}O_{56}\cdot 0.9R^{3+}\cdot 15(H_2O+OH)$. This is approximate because of the presence of impurities in the bulk sample. The presence of magnesium in the framework at this level is consistent with the two main resonances in the ^{31}P MAS NMR (δ −20.5 and −25.4) being due to phosphorus with second nearest neighbor coordination of (3Al, 1Mg) and (4Al), respectively.

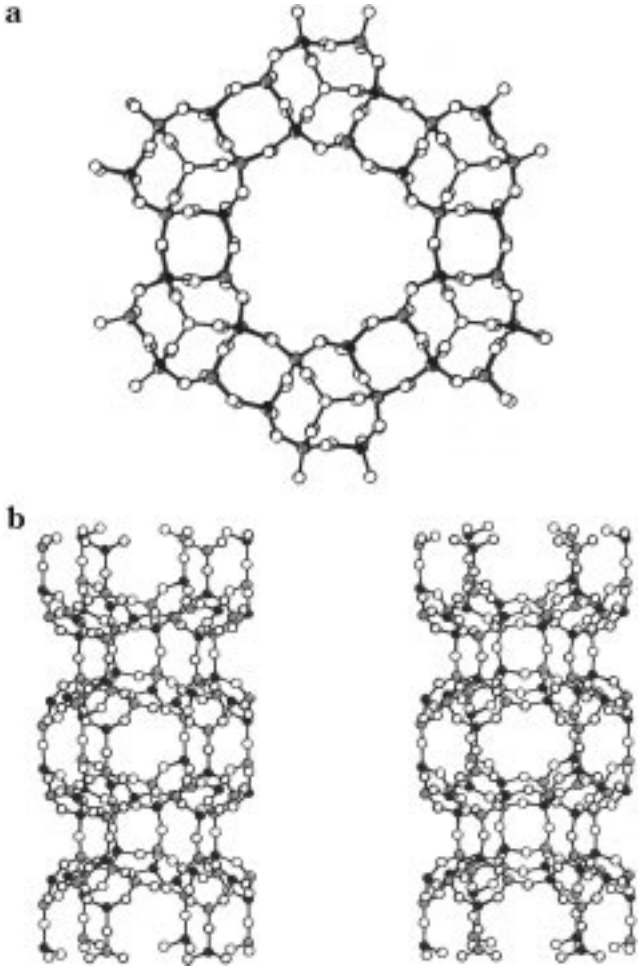

Figure 3. (a) The projection of the STA-5 structure down [001], showing the 12-membered rings that limit the pore space. (b) A stereoview of the one-dimensional channel system in STA-5, showing the supercage and channel arrangement.

X-ray diffraction of STA-1 and STA-5 samples that had been heated in oxygen and then cooled in the presence of cyclohexane vapor revealed that although the structure of STA-1 is largely lost upon calcination, STA-5 remained highly crystalline (Figure 7) and is therefore expected to be active in the catalytic cracking of hydrocarbons, as the related MAPO-46 is found to be.[16] Note that the impurity peaks that are excluded in the Rietveld refinement disappear upon calcination, indicating that the impurity phase is not thermally stable to 550 °C. Prolonged exposure of the sample to moist air results in a major loss of crystallinity.

The synthesis of STA-5, a novel magnesioaluminophosphate that possesses the BPH topology, is of interest not only because it is a good example of the role triquaternary cations can have in the synthesis of new structures, but also because it may throw light on the way aluminophosphate structures assemble from solution. The structure of STA-5 contains the same alumi-

(16) Akolekar, D. B.; Kaliaguine, S. *J. Chem. Soc., Faraday Trans.* **1993**, *89*, 4141.

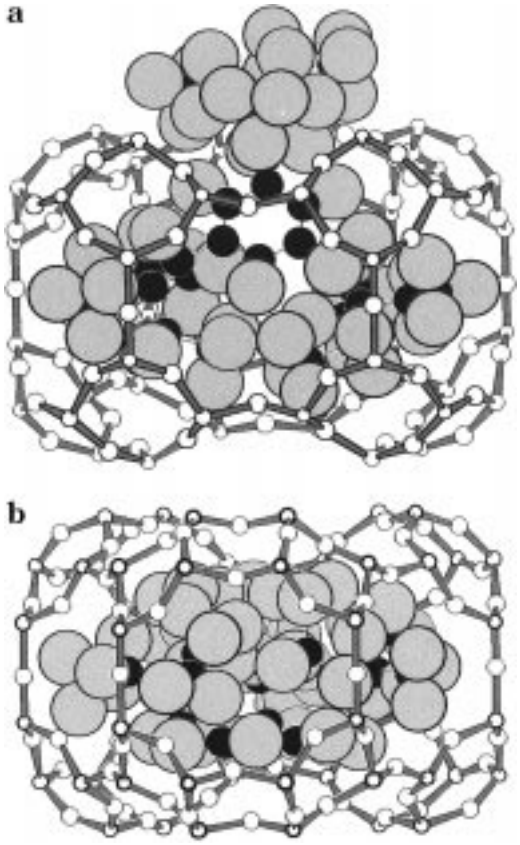

Figure 4. The two lowest energy configurations for template molecules in the STA-5 framework. The hydrogens are represented by the larger gray spheres, the carbon as black spheres, and the nitrogen as dark gray spheres. In part a, the lowest energy configuration is shown, where the template extends out of the supercage, whereas in part b the template is included completely within the supercage.

nophosphate sheets as MAPO-46, but arranged differently. Starting from the same arrangement of a first sheet, the next sheet can join on in two possible ways, which are related by a 60° rotation around the *c*-axis. One results in the AFS tetrahedral net whereas the other results in the BPH topology. Ozin discussed the synthesis of aluminophosphate-based structures in terms of the polymerization of aluminophosphate units into chains, sheets, and frameworks, and the sheets observed in MAPO-46 (and STA-5) were proposed as possible configurations on this pathway.[17] It was therefore to be expected that these sheets could link up during synthesis in the two possible ways described above, especially in the light of the observed occurrence of the BPH topology in beryllophosphate and aluminosilicate topologies. The high crystallinity of STA-5 indicates that there can be few stacking faults and there is no evidence of MAPO-46 as an impurity. It is tempting, therefore, to speculate that the STA-5 stacking sequence crystallizes in preference to the MAPO-46 structure as a result of the geometry of the triquaternary template.

Note: Additional information on the computer-simulated template location in STA-5 is available from the authors.

Conclusions

The synthesis of STA-5 emphasizes the success of the method of rational design and synthesis of organic

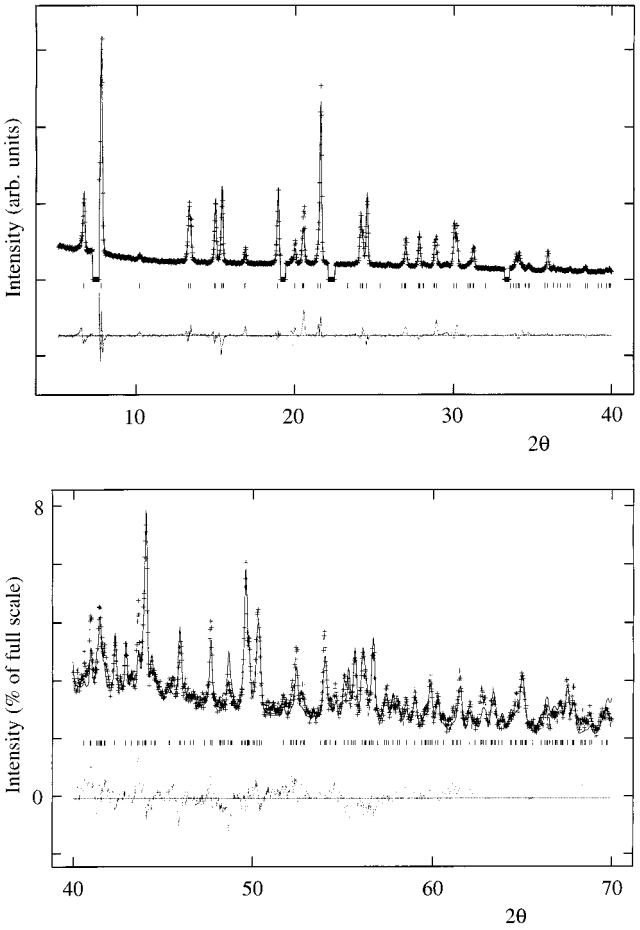

Figure 5. X-ray Rietveld profile fit and difference plot, over two 2θ ranges, of the as-prepared STA-5, including template molecules in the lowest energy configuration with an occupancy of one molecule per supercage. Small Bragg diffraction maxima of a crystalline impurity are excluded by excluding the 2θ regions 7.2−7.6°, 19.1−19.42°, 22.1−22.5,° and 33.2−33.5°. The final R_{wp} is 0.098, with $a = 13.221(1)$ Å, $c = 13.339(1)$ Å.

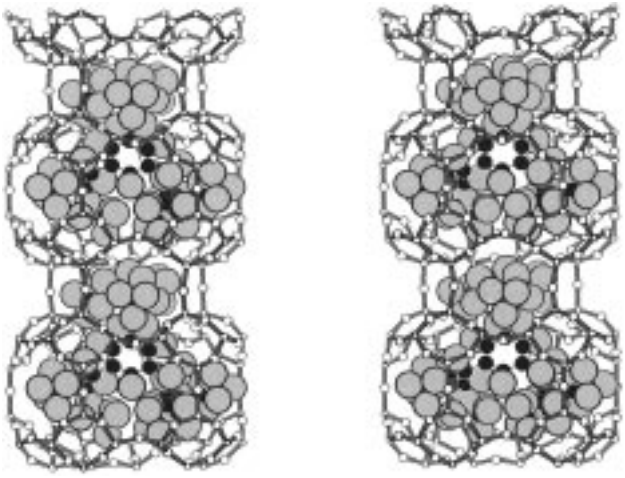

Figure 6. Stereoview of the template within the channel system, as determined from computational simulation and X-ray diffraction measurements.

cations as template molecules. In this case the design is on the basis of the necessity of producing a structure

(17) Oliver, S.; Kuperman, A.; Ozin, G. A. *Angew. Chem., Intl. Ed.* **1998**, *37*, 47.

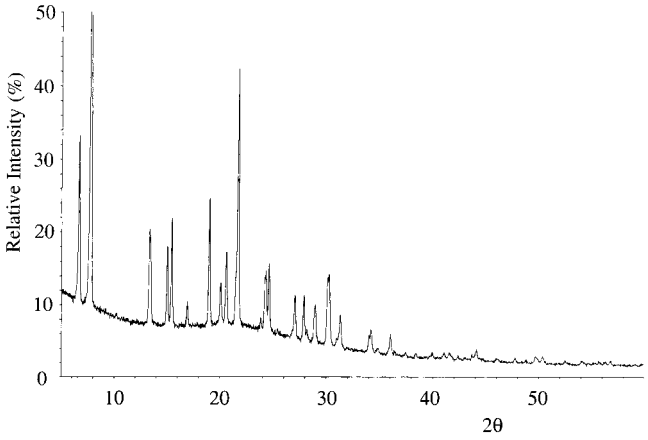

Figure 7. X-ray diffraction profile of calcined STA-5, heated at 550 °C in dry oxygen to remove the template and cooled below 200 °C in dry nitrogen saturated with cyclohexane vapor at room temperature. The refined unit cell is *P*321, with a = 13.20(1) Å, c = 13.31(1) Å.

with desired characteristics if a template of a certain shape is included, rather than the parallel approach of designing a template for a particular structure.[18] STA-5 has linked supercages that accommodate the template molecules. The structure of STA-5 is related to that of MAPO-46, and it is likely that the same general synthesis route is involved, the ultimate mode of crystal growth being controlled by the template.

The approach of modeling the location of template molecules within zeolitic structures is again shown to be a useful one. Previous examples indicated that the predicted template location is often very close to the true position, as determined from powder or single-crystal diffraction data.[19] In addition to helping predict which template may be useful in the synthesis of a desired structure, it enables a higher degree of confidence in structural assignment of open framework solids containing disordered templates that cannot readily be located by difference Fourier methods. For STA-5, good agreement of simulated and measured X-ray powder diffraction data is obtained only by inclusion of the template. The powder diffraction profile is found to be affected more than the single crystal data collected in this work, because the reflections at higher d spacings are much more sensitive to the presence of templates. These low index reflections are collected routinely in powder diffraction but not in microcrystal diffraction, where shorter wavelength X-rays are more commonly used.

Finally, the competitive cocrystallization of MAPO-5 or other phases is difficult to prevent under these conditions, and must occur either without template or in the presence of small fragments that have come from the template via reactions such as the Hofmann elimination. When the triquaternary templates are incorporated in the growing aluminophosphates, they clearly play an important role in producing large pore structures, and vindicate the general approach taken here. For STA-1, the template must be incorporated within the spacious intersections of large pore channels ringed by 12-membered rings, and in STA-5 the bulky template is incorporated within the supercages as shown above. The ongoing design of tri- and even tetraquaternary alkylammonium templates with partially rigid geometries therefore remains an attractive route for the synthesis of novel microporous solids with desired pore sizes and shapes.

Acknowledgment. We gratefully acknowledge the support of EPSRC for this work. We thank Dr. D. P. Tunstall for assistance in MAS NMR characterization and Miss Z. A. D. Lethbridge and Mr. D. A. Wragg for help in collecting the microcrystal diffraction data.

CM991032S

(18) Lewis, D. W.; Willock, D. J.; Catlow, C. R. A.; Thomas, J. M.; Hutchings, G. J. *Nature* **1996**, *382*, 604.

(19) Stevens, A. P.; Gorman, A. M.; Freeman, C. M.; Cox, P. A. *J. Chem. Soc., Faraday Trans.* **1996**, *92*, 2065.